


An efficient computerized decision support system for the analysis and 3D visualization of brain tumor

Irfan Mehmood¹ · Muhammad Sajjad² ·
Khan Muhammad³  · Syed Inayat Ali Shah⁴ ·
Arun Kumar Sangaiah⁵ · Muhammad Shoaib² ·
Sung Wook Baik¹

Received: 15 August 2017 / Revised: 16 April 2018 / Accepted: 17 April 2018 /
Published online: 15 June 2018
© Springer Science+Business Media, LLC, part of Springer Nature 2018

Abstract The quality of health services provided by medical centers varies widely, and there is often a large gap between the optimal standard of services when judged based on the locality of patients (rural or urban environments). This quality gap can have serious health consequences and major implications for patient's timely and correct treatment. These deficiencies can manifest, for example, as a lack of quality services, misdiagnosis, medication errors, and unavailability of trained professionals. In medical imaging, MRI analysis assists radiologists and surgeons in developing patient treatment plans. Accurate segmentation of anomalous tissues and its correct 3D visualization plays an important role in appropriate treatment. In this context, we aim to develop an intelligent computer-aided diagnostic system focusing on human brain MRI analysis. We present brain tumor detection, segmentation, and its 3D visualization system, providing quality clinical services, regardless of geographical location, and level of expertise of medical specialists. In this research, brain magnetic resonance (MR) images are segmented using a semi-automatic and adaptive threshold selection method. After segmentation, the tumor is classified into malignant and benign based on a bag of words

✉ Muhammad Sajjad
muhammad.sajjad@icp.edu.pk

Khan Muhammad
khan.muhammad.icp@gmail.com

¹ Department of Software, Sejong University, Seoul, Republic of Korea

² Digital Image Processing Laboratory, Department of Computer Science, Islamia College Peshawar, Peshawar, Pakistan

³ Intelligent Media Laboratory, Digital Contents Research Institute, Sejong University, Seoul, Republic of Korea

⁴ Department of Mathematics, Islamia College Peshawar, Peshawar, Pakistan

⁵ School of Computing Science and Engineering, VIT University, Vellore, India

(BoW) driven robust support vector machine (SVM) classification model. The BoW feature extraction method is further amplified via speeded up robust features (SURF) incorporating its procedure of interest point selection. Finally, 3D visualization of the brain and tumor is achieved using volume marching cube algorithm which is used for rendering medical data. The effectiveness of the proposed system is verified over a dataset collected from 30 patients and achieved 99% accuracy. A subjective comparative analysis is also carried out between the proposed method and two state-of-the-art tools ITK-SNAP and 3D-Doctor. Experimental results indicate that the proposed system performed better than existing systems and assists radiologist determining the size, shape, and location of the tumor in the human brain.

Keywords Medical image processing · Tumor segmentation and classification · MRI images · Medical imaging · MRI 3D visualization

1 Introduction

Medical imaging is an enthusiastic field of research from the last few decades contributing to society in a number of ways. There are various imaging modalities in the medical field, such as MRI, CT scan, endoscopy, and so on. These imaging modalities play a vital role in current medical procedures for research studies, diagnosis, and treatment of multifactorial medical diseases. In the current era, medical imaging plays an important role in the performance of any radiology department. Medical images need image processing techniques such as image enhancement and segmentation [34] to find out diagnostic statistics such as detection of disease or its level of severity. Human brain analysis is one of the hottest research areas for biomedical and computer scientists [16]. The brain is the main organ of human body, protected by a bone called a skull. The average weight of a normal brain is 1300–1500 mg with a volume of 1260 cm³. The human brain consists of 86 billion neurons, blood vessels, and glial. It can be divided into the gray, white, and cerebrospinal fluid. The white matter appears as a pinkish white color and it is covered by gray matter due to the absence of myelin sheath. The color of gray matter appears as a light gray and can be easily distinguished from white matter. The brain in the skull is surrounded by cerebrospinal fluid that is also spread throughout the length of spinal cord. Brain tumor/anomaly is an abnormal growth of tissues. The cells in the living organism die and are replaced with new cells, but when a tumor occurs the cells grow and do not die, threatening life. The tumor can be broadly divided into two classes, benign and malignant, i.e., a benign tumor is a non-cancerous tumor and these are smaller in size, slow in growth, and do not spread to the nearby normal cells. However, malignant tumors are cancerous, large in size, and fast growing.

Magnetic resonance (MR) imaging is the most popular and effective modality for brain analysis. It creates 3-dimensional (3D) DICOM images of the soft tissues. MR imaging machines generate volumetric images (T1W, T2W, FLAIR, and proton density), assisting the radiologists to study human organs in detail. Manual analysis of brain MRI is time-consuming and prone to errors due to the nature of complexity and size of MRI data for each patient. In this context, various state-of-the-art segmentation techniques have been presented; each method carries some advantages along with limitations [11, 22, 23]. A majority of the work in current literature has been performed on a single 2D slice of volumetric images. Segmentation in a single slice in comparison of volumetric data is easier, but results are not satisfactory. The segmentation of tumor is carried out for numerous purposes such as volume calculation, 3D visualization, and classification of a brain tumor [17]. Manual thresholding is one of the most

popular methods for the segmentation of DICOM volumetric data [25]. Performance of threshold-based segmentation methods depends on the selection of appropriate threshold value.

Manual selection of the best threshold is very challenging and requires extensive expertise [4]. In this regard, Otsu binarization automatically segments different parts of the human brain and tumor by automatically selecting threshold values [3]. Otsu binarization method is easy to implement but it is not robust to noise and suffers during segmenting tumors having a similar texture to other brain parts. Watershed [28] is another segmentation algorithm that is suitable for segmenting overlapping objects, which applies watershed and gradient magnitude to segment tumors or objects of interest. Watershed method's overall performance is good, but its results for 3D volumetric segmentation are not satisfactory. Clustering is an unsupervised learning technique in machine learning used to group unlabeled objects with similar properties in a cluster [9]. Among clustering algorithms, K-means is a well-known clustering algorithm that can be used for image segmentation and clustering categorical data [2]. Region growing [10] is also a popular image segmentation method that is based on seed points. A seed point is the starting point from where it starts to grow, and a homogeneity criterion is followed to group the neighboring pixels into the same region. Different seed points for the same region can provide different results. Region growing method is a semi-automatic method for segmentation, where selecting a good seed point is a challenging task. Fuzzy C-mean (FCM) [19] is also a widely used clustering algorithm similar to K-means but FCM is computationally more complex than K-means segmentation [13].

The proposed work is the extension of our MRI analysis methods: prioritization of brain MRI and anisotropic diffusion based brain MRI segmentation [22]. In current work, K-means is used to cluster the region of different tissues containing in DICOM volumetric images, where the value of K represents the number of different brain tissues: tumor skull, white matter, gray matter, and cerebrospinal. Before applying K-means, intensity values of volumetric images are first converted into a one-dimensional array as a pre-processing step. After segmenting the brain into different tissues, classification is performed to analyze the category of each tissue as to whether is infected or not. In our case, the purpose of classification is to develop an efficient system to categorize tumor across different pathological types. BoW features extraction method was originally used for the classification of object category and usually does not give satisfactory results over the images containing geometrical transformation inconsiderable amount, e.g., rotation and translation. MR images contain geometrical transformation in large amount. Thus in the proposed work, BoW is amplified by SURF features for effective classification of a brain tumor for which training images of benign and malignant tumors were obtained along with their ground truth. After segmentation and classification, the volume of the brain is calculated using the information obtained from the DICOM header. Further, the area of the segmented brain and tumor is calculated using the regional properties. In computer graphics volume rendering is a technique of creating 3D models from a series of 2D images. In the proposed framework, marching cube algorithm is used [20] for volume rendering of segmented brain and tumor images as it helps us to visualize the location, shape, and size of the tumor in the brain. The key contributions of the proposed framework are summarized as follows:

1. An efficient framework for region of interest (ROI) segmentation, classification, and visualization is proposed, where features extraction for training and classification is an offline process and can be replaced by any efficient features extraction and classification technique. In addition, the segmentation method can be easily added or removed and ROI

- can be visualized using any efficient visualization technique replacing marching cube algorithm.
2. A semi-automated, interactive technique is proposed for MR image segmentation which selects the optimum threshold values.
 3. The volume of brain and tumor is calculated by retrieving the information of pixel spacing and slice thickness from the DICOM header, the regional properties of the segmented brain and tumor help us to calculate the number of voxels.
 4. The BoW feature extraction method is amplified via SURF incorporating its procedure of interest point selection, and then the labelled features are classified into benign or malignant using SVM classifier.

The rest of the paper is organized as follows: Section 2 summarizes the literature review; Section 3 introduces the proposed framework; Section 4 describes the experimental setup and performance evaluation; Section 5 concludes the paper.

2 Literature review

In this section, the literature is covered from a different perspective, i.e., segmentation, classification, and visualization so that readers can easily grip the concepts behind the proposed work. Segmentation techniques with some pre-processing operations are described, followed by classification. The reason is that segmenting ROI on which classification is carried out, is prerequisite not only for classification but also for visualization. Lastly, visualization is briefly presented taking some valuable work from the literature.

In [25], authors presented a very basic and helpful framework for MRI enhancement and segmentation. In a pre-processing step, the image is enhanced using histogram equalization and morphological operations are applied to remove unwanted blobs. The median filter is also applied to remove noise from MRI images. Finally, threshold-based segmentation is applied to detect the tumor. This technique provided better results than semi-automatic and automatic segmentation, however, it is computationally expensive due to manual selection of an appropriate threshold. Zhang et al. presented a concise survey of existing techniques related to brain MRI analysis along with discussing various segmentation algorithms for brain tumor segmentation [34]. There are various threshold-based segmentation methods ranging from manual to automatic thresholding, each having its own pros and cons. For example, Otsu thresholding is a segmentation technique that automatically selects the best threshold value using intra-class variance between foreground pixels and background pixels. Region growing is another well-known segmentation algorithm based on seed point selection. The growth of the seed point is based on homogeneity criteria. This algorithm provides good results, but it is very sensitive to noise, contrast variation, and selection of suitable seed point. Khotanlou et al., [19] proposed fuzzy clustering algorithm for segmenting 3D MR data, which is similar to K-means. Fuzzy segmentation method divides voxel into two classes incorporating a finite number of fuzzy levels for each class. The complexity of fuzzy segmentation method is more than K-means and other segmentation algorithms, making it computationally expensive compared to other methods.

In [10], authors presented brain tumor segmentation scheme that uses region growing algorithm along with gradient and variance, overcoming the challenges of manual thresholding. In this method, the information of edges are preserved, then the mean-variance

of the boundary curve is calculated. These two descriptors are used for automatic selection of threshold value, which in turn is by the region grow segmentation algorithm. According to authors, better results for tumor segmentation were achieved using this approach. In [31], authors presented an automatic method that is more accurate in the segmentation of white matter, gray matter, and CSF from 3D MRI images. This method consists of three steps: first histogram based segmentation is performed, then texture features are extracted, and finally, SVM is used for classification. In [29], authors claimed a fully automatic brain tumor segmentation framework for 3D T1W MRI data. They, first normalized Gaussian mixture method to model normal brain and then a 2D fluid vector flow (FVF) algorithm is extended to 3D FVF. This method is tested on a local dataset with satisfactory experimental results for brain tumor segmentation.

In [18], an automatic segmentation technique based on a statistical approach using tissue probability maps is presented that automatically recognizes the class of tumors. The method is tested on two standard brain tumor datasets (i.e., BRATS 2013 and Leaderboard¹). In [32], the tumor is classified by extracting shape features (that is, eccentricity, solidity, difference area-hull-rectangular, difference area-mass-rectangular, cross-correlation left, and cross-correlation right) along with texture features of the extracted ROI. SVM is trained over features extracted from training images in the previous phase and a class label is assigned to new data (i.e., benign or malignant) while testing it over the previously trained SVM. Authors have claimed 95% accuracy. In [30], the author presented a wavelet-energy based approach for automated classification of MR brain images as normal or abnormal. SVM was used as the classifier, and biogeography-based optimization (BBO) was introduced to optimize the weights of the SVM. The results based on a 5 fold cross-validation showed the performance of the proposed BBO-KSVM was superior to BP-NN, KSVM, and PSO-KSVM in terms of sensitivity and accuracy. Classification performance depends on the selection of suitable features such as GLCM [33], Gabor filter [16], and wavelet transform [2]. SVM is widely used to identify normal and abnormal brain MRI [33]. BoW features extraction method for tumor classification and medical image retrieval [10, 27] provide more robust results. The bow is also very efficient for the organ classification in X-Rays images [10] and for classification of breast tissues in mammogram images [19].

Y. Chen in [7], proposed a technique for performing segmentation and rendering of both the brain and tumor regions. A 3D Bayesian level set method is used to segment brain and tumor from its 3D data. Segmented slices are used by the ray casting algorithm to render 3D models of the brain and tumor. In [8], the author presented a new 3D volume rendering technique, computing volume of brain and tumor from MR and CT images. 3D widgets and volume clipping are combined with volume rendering. 3D widgets are used to calculate the area, distance, and angle of the objects. M. Bozorgi and F. Lindseth in [6] developed a GPU based ray casting volume rendering algorithm in VTK. CPU based ray casting algorithm can produce high-quality 3D images from 2D series, but such algorithms are constrained by time complexity. Rendering time can be reduced using GPU based ray casting algorithm developed in VTK library.² This method is platform independent and can be run over different GPUs. In [1], a GPU based Fourier volume rendering method was presented, which is widely used for 3D reconstruction of medical data. This GPU based Fourier volume rendering technique is faster than spatial domain based rendering algorithms, achieving a speed of 117× faster than CPU.

¹ https://figshare.com/articles/BRATS_2013_Leaderboard_and_Test_Datasets/1348692

² <http://www.vtk.org/>

3 Methodology

The proposed framework consists of four steps: 1) estimation of an efficient threshold for segmentation of brain tissues, 2) volume calculation of the segmented regions of interest, 3) classification of segmented tumor into benign or malignant using SVM classifier over SURF inspired BoW features, and 4) 3D visualization of ROI using marching cube algorithm. For robust segmentation, a semi-automated threshold selection method is presented, producing optimal results for segmenting brain DICOM data. In feature extraction phase, BoW is adopted to extract interest points from images using SURF descriptor and to make a dictionary of the SURF points. SVM is trained for classification. The volume of brain and tumor are calculated, considering the Meta information provided in DICOM header (pixel spacing and slice thickness etc.). The regional properties of the segmented brain and tumor allow calculating the total number of the voxel, which helps in measuring the volume of the brain and tumor. It is important to mention that voxel is a primitive 3D element in MRI and it is calculated in mm^3 . The last module of the proposed work is 3D visualization. Segmentation is the prerequisite of visualization, hence segmented regions of brain and tumor are imported by the marching cube algorithm to render a 3D model from series of 2D segmented DICOM slices. The overall view of the proposed framework is shown in Fig. 1.

3.1 Brain and tumor regions segmentation

Segmentation is the process of partitioning a digital image into multiple segments (sets of pixels, also known as super-pixels). The goal of segmentation is to simplify and/or change the representation of an image into something that is more meaningful and easier to analyze. In segmentation, optimal threshold selection is the vital parameter, which is the most challenging and usually time-consuming task. In the proposed method, the input brain MR slice is displayed via GUI component to the user, making five random clicks over both tumor region and non-tumor region. The pixel values of the clicked points are saved in a vector and are utilized to estimate the darkest and brightest threshold of the corresponding tissue (brain or tumor) incorporating minimum and maximum intensities, respectively. However, it is not guaranteed that users' selected points belong to darkest or brightest regions. To overcome this problem, a tolerance rate is used and its value is added to the maximum threshold value which in turn is then subtracted from the minimum threshold value. Tolerance is an intensity dependent parameter, which is sensitive to the input MR image. It has been observed that tolerance value of ten is the most suitable value for 8-bit MR images (with 0–255 intensity range). Tolerance value increases while dealing with higher intensities ranges and vice versa. However, it can be adjusted according to the underlying intensity levels. For example, tolerance value can be approximately 2000 while working on a 16-bit MR image having intensity in the range 0 to 65,535. In the current scenario, we are mainly focusing on 8-bit MR images, thus the tolerance value is ten. The proposed segmentation method is applied to volumetric DICOM data as shown in Fig. 2.

After segmentation, morphological operations (erosion/opening) are used as post-processing steps to remove irrelevant and noisy objects from segmented brain and tumor as shown in Fig. 3. Morphological operations are based on structuring element (SE). Each voxel value is matched with SE by incrementing the voxel location for the purpose hitting the voxel

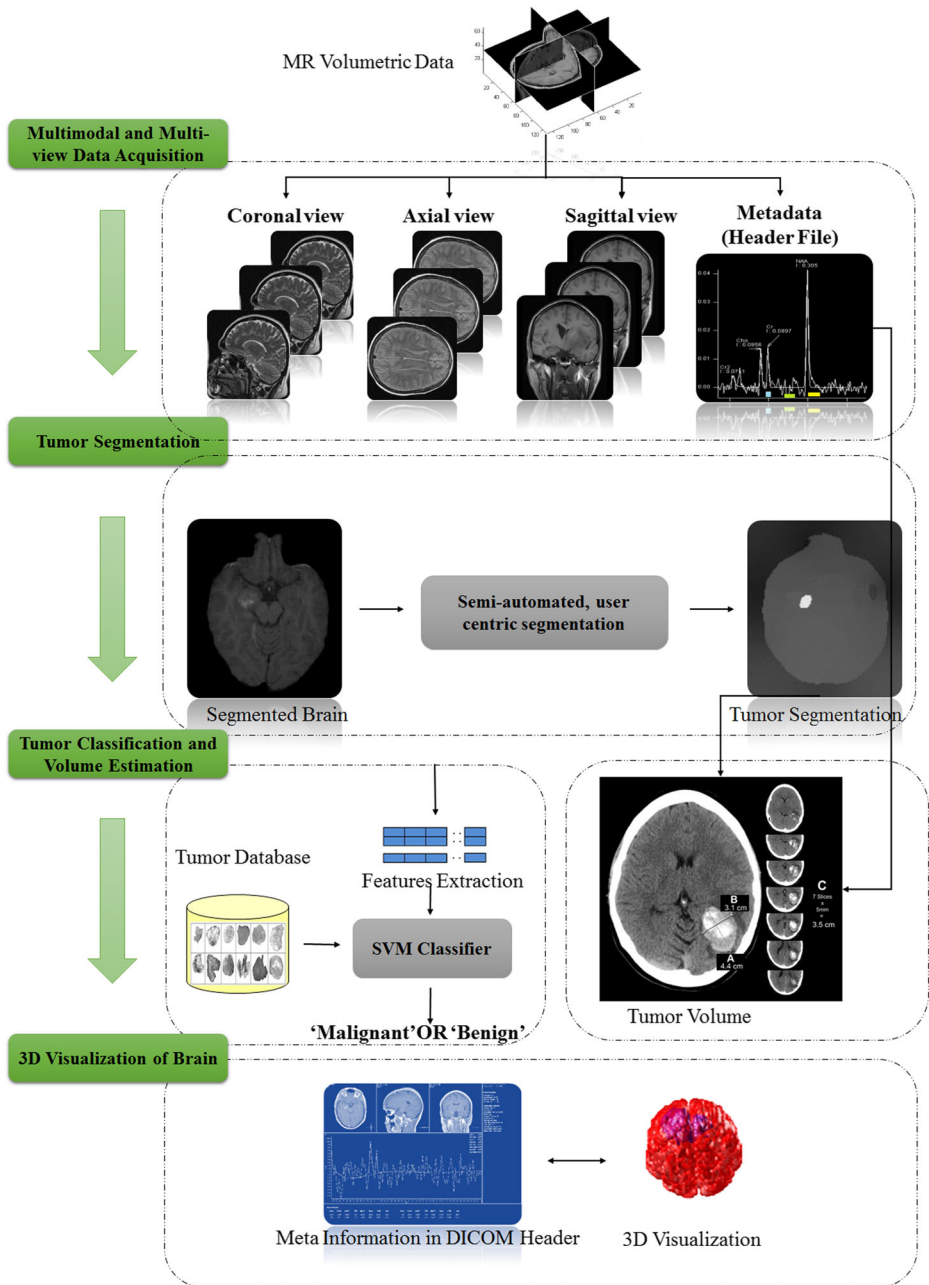


Fig. 1 An overview of the proposed computerized decision support system for the analysis and 3D visualization of brain MRI

at the center of SE. 2D SEs are either a square grid of eight neighbor pixels of square shape or a square grid of six neighboring pixels forming a cross shape. 3D SE is similar to 2D with an additional Z-plane as given in Fig. 4. In 2D SE, the center pixel has 4 or 8 neighboring pixels

Radiologists five clicks on brain and tumor regions for three different brain views

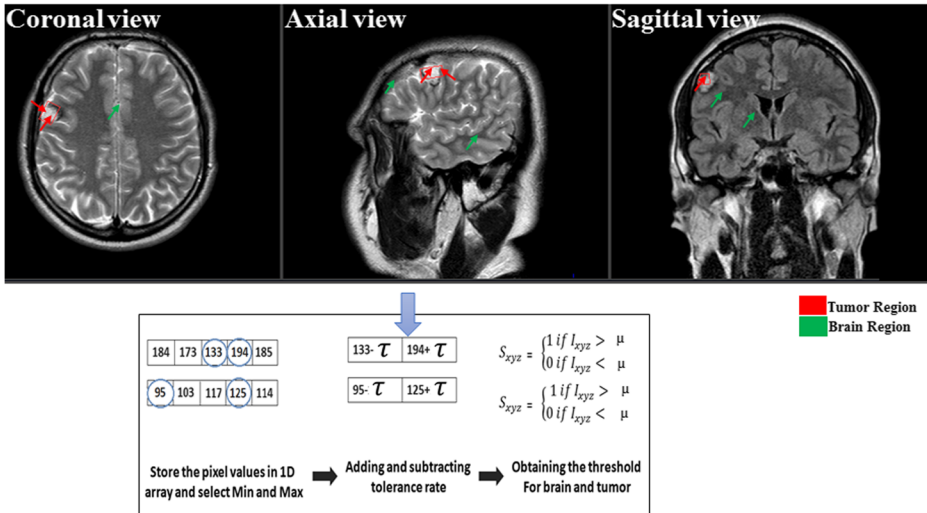


Fig. 2 Semi-automatic intensity-driven and interactive threshold selection method

while in 3D, the center voxel may have 6, 18 or 26 neighboring voxels. For instance, if we create a 3D cube filter of ones (3 3 3), the first 3 refers to the number of voxels in X-axis, the second 3 is the number of voxels in Y-axis, and the remaining is for a number of slices in the volumetric data.

3.2 Segmented object size calculation

Brain and tumor volume can be calculated by computing the tumor area using regional properties of the objects. In order to measure the size of a tumor from MR volumetric data, we need to compute the area of the tumor and brain followed by calculating their volume. In our case, the number of voxels of an object indicates its area. Tumor volume calculation is one of the most important information for radiologists and surgeons. We first calculate brain and tumor area, followed by voxel size calculation as shown in Figs. 5 and 6. Voxel size is calculated in cubic millimeter obtaining pixel spacing in millimeter and slice thickness in

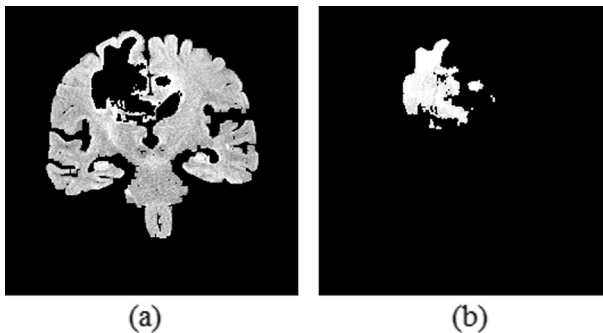


Fig. 3 a Morphological eroded brain. b Morphological eroded tumor

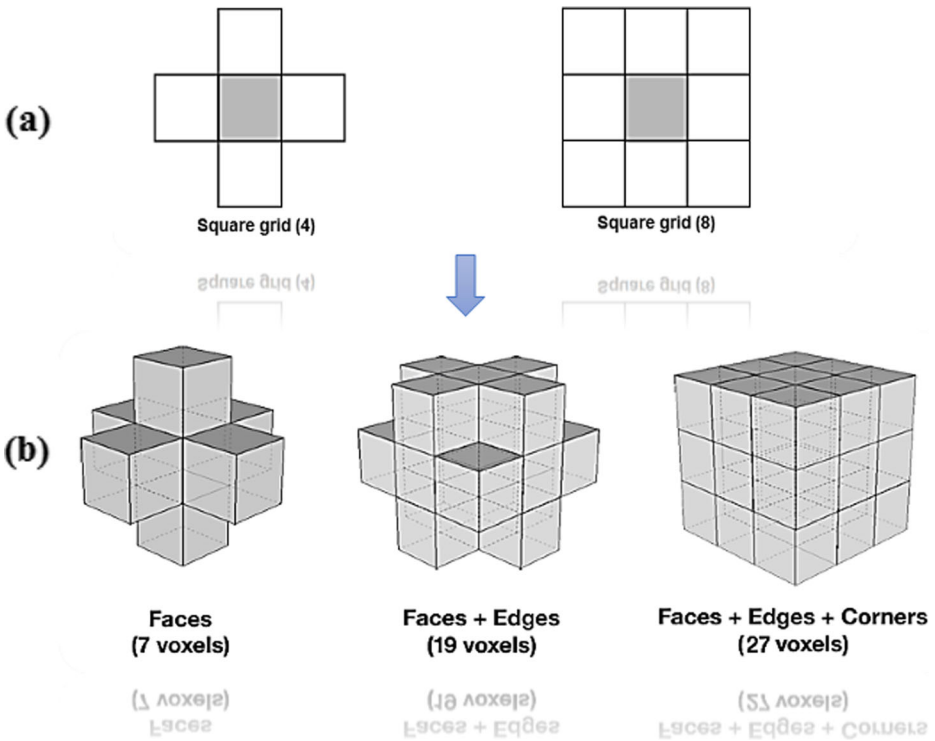


Fig. 4 a 2D structuring elements. b 3D structuring elements

millimeter from the DICOM header. Voxel size V , the area of brain V_B , and tumor V_T are calculated as follows:

$$V_{i,j,k} = mmPerPixelX * mmPerPixelY * mmPerPixelZ \tag{1}$$

$$V_B = A_B * V_{i,j,k} \tag{2}$$

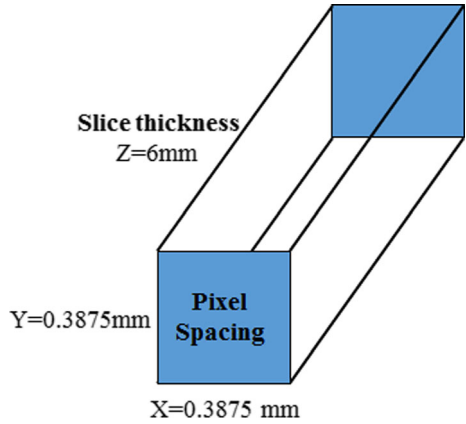
$$V_T = A_T * V_{i,j,k} \tag{3}$$

Where $mmPerPixelX$, $mmPerPixelY$ and $mmPerPixelZ$ represent millimeter per pixels in X, Y and Z direction, respectively in 3D voxel as shown in Fig. 5.

3.3 Features extraction and brain tumor classification

The World Health Organization (WHO) has made a new tumor classification system in 2016 which is used by most of the medical institutions around the world [21]. This classification of WHO is based on the locality of (body parts) tumor (where it resides) and rate of its growth. According to this classification, there are 120 types of brain tumors either belonging to the benign or malignant category. A benign tumor grows slowly and does not spread to other parts,

Fig. 5 Voxel with pixel spacing and slice thickness



having very clear edges with a very little effect on the human body. Such types of tumors can be serious if they are located in the brain. Malignant tumors have different structures than benign and are also known as brain cancer. The common symptoms of tumors are hearing loss, dizziness, walking, and balancing problem. Classification is the process to assign a class label to the testing data. The first phase of classification problem is to train the model. The accuracy of a trained model depends on quantity and heterogeneity of training data, features used for classification, and classifier’s kernel function. In our current scenario, classification is performed on segmented tumor regions. Tumor volume is saved into its 2D image slices and used for features extraction and classification purposes. For classification, SURF enhanced BoW features are extracted. The working mechanism of SURF features are similar to SIFT but are faster and robust than SIFT.

SURF algorithm is implemented in three phases. In the first phase, points of interests (POIs) are selected for which hessian matrix is adopted. In the second phase, local neighborhood descriptors are used to describe pixel intensity distribution in the neighborhood of the POIs. In

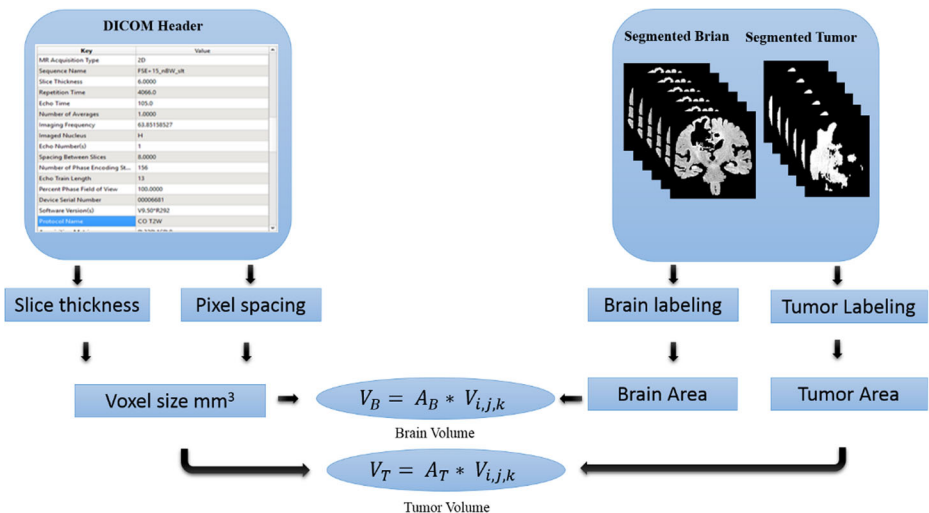


Fig. 6 Volume calculation of brain and tumor from volumetric data

the third phase, different features are compared that are obtained from different images and matching pairs. PoIs selection is done using a grid with 8×8 spacing. A vector consisting of 32 pixels is created, where each element of the vector corresponds to a square block from where SURF features are extracted. Multiple square blocks are used to extract multi-scale features. PoIs are stored in feature vectors and these features are quantized using k-mean clustering algorithm. By default, the number of clusters used by a bag of feature is five hundred that can be increased or decreased. Visual words are the centers of the clusters and vocabulary is the combination of all visual words. Features in vocabulary are categorized and a visual word is used to represent the category as shown in Fig. 7. An encoding method is used for counting visual words occurrences in an image and a histogram of the image is created.

The proposed method uses SVM to classify tumor into benign or malignant. SVM is trained using the error correcting output codes framework and a bag of features are utilized to encode images from the training set into a histogram of visual words. These histograms are then used to train the classifier. Each image from the training dataset is encoded using the encoding scheme of bag of features algorithm. Features from each image are detected, extracted and then a feature-histogram for each training image is created with the help of an approximate nearest neighbor clustering algorithm. The length of the histogram is dependent on the number of visual words and the feature vector created from the histogram. The overall view of the proposed tumor classification is shown in Fig. 8. In this work, SVM selects a hyperplane between two classes of the training data that has maximum margin. Many hyperplanes can be drawn to separate the two classes and SVM selects the optimal hyperplane, which can be defined as follows:

$$Wx + b = 0 \tag{4}$$

Herein, x is a point on the hyperplane, representing normal to the hyperplane and b is the bias. $\|W\|$ is the mean of the Euclidean. Hyperplane for separating two classes in case of linear separability can be defined as follows:

$$wx_i + b \geq +1, y_i = +1 \tag{5}$$

$$wx_i + b \leq -1, y_i = -1 \tag{6}$$

$$y_i (wx_i + b) - 1 \geq 0 \tag{7}$$

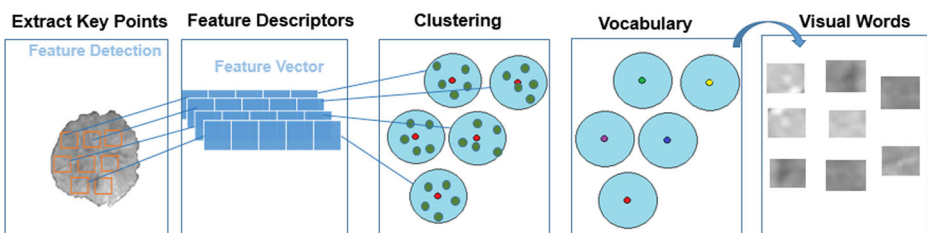


Fig. 7 Feature extraction using BoW

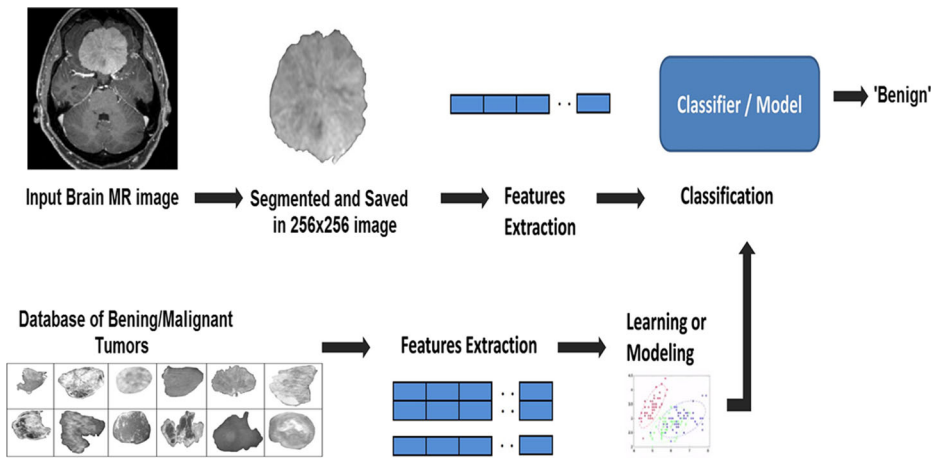


Fig. 8 The proposed brain tumor classification framework

The error correcting output code framework is a multi-class model that reduces three or more classes to binary class. The proposed method uses a coding design known as one vs one. To avoid cluttering, readers are referred to [5, 24] for further details on the binary classification via multi-class model using error correcting output.

3.4 3D reconstruction of brain tumor

3D reconstruction is the transformation of 2D images to a 3D brain view. Quality of the 3D model depends on the number of slices in DICOM series as shown in Fig. 9. For 3D visualization, marching cube algorithm is incorporated using divide and conquer approach for the creation of 3D high-resolution surface. Cubes are created between two adjacent slices [20], where each cube consists of 8 vertices, hence there are 256 ways that a surface can

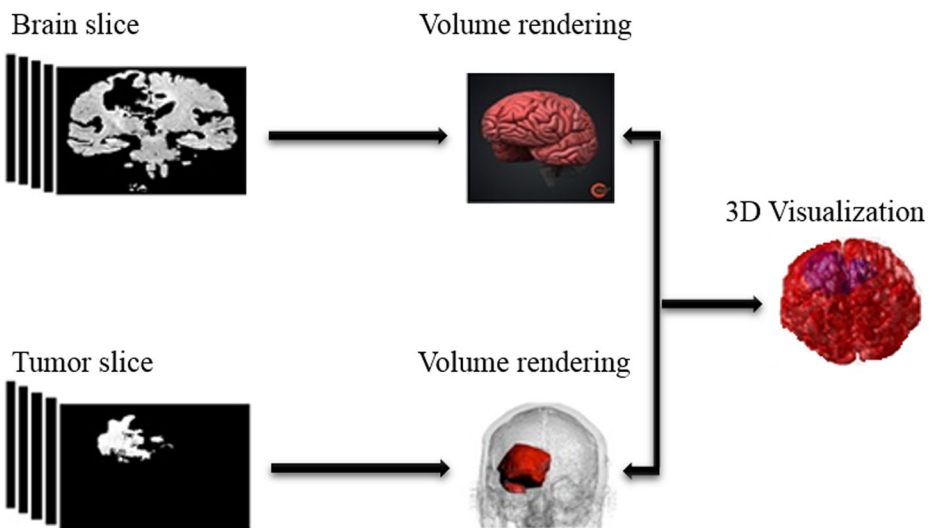


Fig. 9 3D visualization flowchart

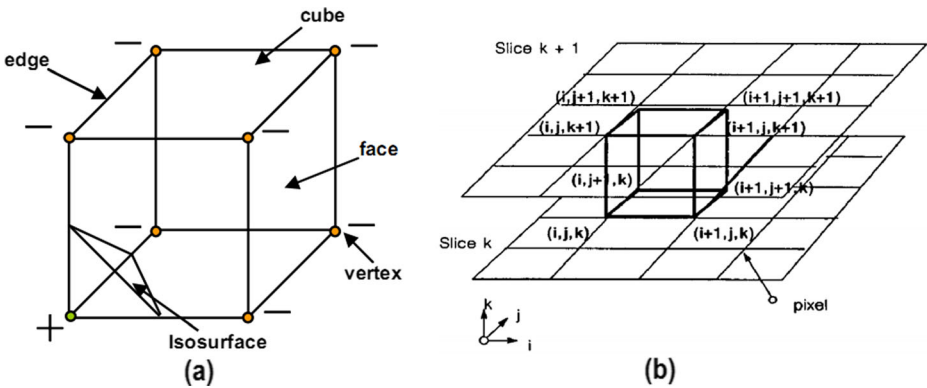


Fig. 10 a A cube and b its two adjacent slices

intersect a cube. These 256 cases are reduced to 14 patterns [25] as mentioned in Fig. 10. These 14 patterns are used to calculate the surface intersection x with cube edges. The gradient of cube vertex (i, j, k) can be estimated as follows:

$$G_x(i, j, k) = \frac{D(i + 1, j, k) - D(i - 1, j, k)}{\Delta x} \tag{8}$$

$$G_y(i, j, k) = \frac{D(i, j + 1, k) - D(i, j - 1, k)}{\Delta y} \tag{9}$$

$$G_z(i, j, k) = \frac{D(i, j, k + 1) - D(i, j, k - 1)}{\Delta z} \tag{10}$$

4 Experimental results and discussion

In order to evaluate the efficiency of the proposed framework, numerous experiments were carried out on different MRI datasets. All the simulations for segmentation, classification, and visualization are implemented using MATLAB 2015. Various standard evaluation metrics were used to analyze the performance of the proposed framework. This section consists of the evaluation of four major parts of the proposed framework, comprehensively assessing each module of the framework.

4.1 Dataset and MRI characteristics

Dataset is obtained from the department of radiology, Lady Reading Hospital Peshawar³ (LRH), Pakistan. Images were acquired through TOSHIBA 1.5 Tesla machine with resolution $640 \times 640 \times 19$ with a bit-depth of 8. The variance in a number of slices, pixel spacing and

³ <http://www.lrh.gov.pk/>

slice thickness provided by TOSHIBA 1.5 Tesla machine is illustrated in Table 1. Radiologists select appropriate values for parameters mentioned in Table 1, considering the nature of disease under diagnosis. To evaluate the proposed framework, 1100 scans having $0.3875 \times 0.3875 \times 6 \text{ mm}^3$ pixels spacing (width and height) and slice thickness, respectively, as mentioned in the first row in Table 1.

4.2 Evaluation of the proposed 3d segmentation method

A subjective performance evaluation of the proposed segmentation method is performed using sensitivity, specificity, and F-measure as given:

$$\text{Sensitivity} = \frac{TP}{TP + FN} \quad (11)$$

$$\text{Specificity} = \frac{TN}{TN + FN} \quad (12)$$

$$\text{FNR} = \frac{FN}{TP + FN} \quad (13)$$

$$\text{FPR} = \frac{FP}{TN + FP} \quad (14)$$

$$\text{F-Measure} = 2 * \frac{FPR * FNR}{FPR + FNR} \quad (15)$$

Herein, true positive (TP) is the number of voxels in the MR image correctly identified as a tumor voxel and false positive (FP) is the number of non-interesting region voxels that are incorrectly recognized as tumor voxels. True negative (TN) presents the number of non-interested voxels which are considered correct as non-interesting voxels. False negative (FN) is the number of voxels that are incorrectly identified as non-interesting ROI voxels. F-Measure is the weighted harmonic mean of false positive rate (FPR) and false negative rate (FNR) which provides a better understanding of the segmentation results. Table 2 shows that F-measure of the proposed segmentation technique is 98%. This indicates that the proposed segmentation results are accurate, and closer to manually segmented brain tumors in MR images. The proposed 3D segmentation algorithm creates a set of solutions over the single result to overcome the trap of local optimum. Figure 11 shows visual results of the proposed 3D segmentation technique.

4.3 Analysis of tumor volume calculation

In a series of DICOM images, total voxels consist of the brain, tumor, vessels, skulls, and background voxels of the volumetric data. Mean intensity is the average voxel intensity of

Table 1 Example brain and tumor volume statistics and voxel information

| No: | Slices | Total voxels | Intensity mean | Intensity standard deviation | Pixel spacing (millimeter) | Slice thickness (millimeter) |
|-----|--------|--------------|----------------|------------------------------|----------------------------|------------------------------|
| 1 | 19 | 7,782,400 | 1536.09 | 1780.89 | 0.3875 | 6.0 |
| 2 | 28 | 2,419,200 | 98.9 | 106.61 | 0.7188 | 5.0 |
| 3 | 19 | 7,782,400 | 1254.66 | 1473.18 | 0.3437 | 6.0 |
| 4 | 28 | 2,544,640 | 112.38 | 143.43 | 0.8125 | 5.0 |
| 5 | 17 | 4,980,736 | 918.15 | 1479.13 | 0.4707 | 7.0 |

each volumetric data. The pixel spacing is the length of a voxel in X-axis and Y-axis in millimeter while the slice thickness is the length of Z-axis of the voxel. The voxel information and volume statistics for MR scan with resolution $640 \times 640 \times 19$ (8 bit-depths) are given in Table 3.

4.4 Comparative analysis of the proposed classifier

Performance of the proposed classifier is measured in terms of confusion matrix, sensitivity, specificity, accuracy, and mean squared error. It can be seen from Table 4 that SVM classifier achieves a minimum mean squared error of 0.09 in comparison with other classification models. It also possesses the highest level of accuracy, proving its effectiveness and reliability. The BoW features amplified via SURF with SVM classifier achieves an accuracy of 99% for the entire test set. For the evaluation of the proposed classifier, we considered the same dataset that is used for the brain and tumor segmentation evaluation. The proposed feature extraction method enhances the performance of SVM classifier which is the most feasible learning model for feature selection over a higher dimension space. Table 4 shows the performance analysis which highlights that the proposed approach achieves better accuracy in comparison with other classifiers [12, 15, 26]. The experimental results show that SVM combined with BoW features yields higher performance in feature selection, optimization, and tumor classification.

Under the supervision of the radiologists, underlying brain MR images dataset was manually labeled as malignant and benign. This ground truth is used for the training of SVM classifier and classification performance is evaluated using the testing dataset which consists of images with a coronal, sagittal, and axial view. Each MR series is confirmed by obtaining the biopsy reports. Cases obtained without biopsy reports were not included in the training dataset. The training dataset was divided into training and

Table 2 Performance comparison of the proposed segmentation method with other three state-of-art techniques using a baseline (ground truth) provided by radiologists

| Method | Sensitivity | Specificity | FPR | FNR | F-Measure |
|--------------------|--------------|--------------|--------------|--------------|-----------|
| BET [33] | 0.999(0.001) | 0.982(0.005) | 0.115(0.063) | 0.675(0.098) | 0.89 |
| Irfan et al. [22] | 0.982(0.03) | 0.991(0.008) | 0.069(0.055) | 0.178(0.076) | 0.88 |
| Haiyan et al. [33] | 0.973(0.01) | 0.993(0.003) | 0.05(0.022) | 0.099(0.097) | 0.96 |
| Proposed method | 0.962(0.01) | 0.995(0.004) | 0.05(0.018) | 0.099(0.098) | 0.98 |

Values in () represents standard deviation

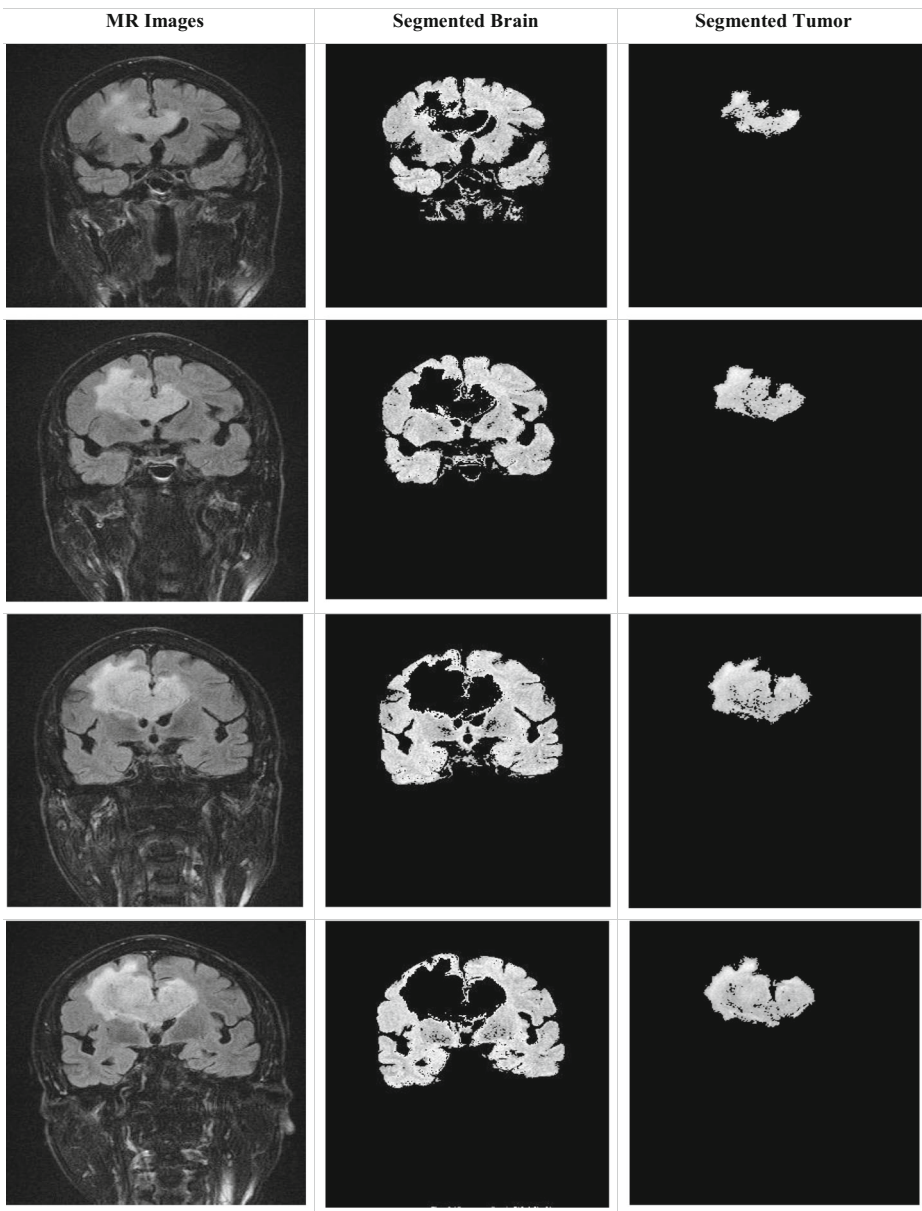


Fig. 11 Visual results of the proposed brain and tumor segmentation method on a sequence of MR scans, showing brain and tumor regions detected from slice to slice

testing using cross-validation of 70% training and 30% for testing as given in Table 5. As the proposed system is based on k-mean clustering with SVM classification followed by volume rendering based 3D visualization. The computational complexities of these approaches are $O(kn)$, $O(n^3)$ and $O(n^2)$ respectively. Where k represents number of clusters and n represented number of samples or instances. The overall complexity of the proposed system will be a linear combination of all the aforementioned complexities.

Table 3 Brain and tumor volume calculation

| No: | Voxel size in cubic millimeters | Total brain voxels | Total tumor voxels | Brain volume in cubic millimetres | Tumor volume in cubic millimetres |
|-----|---------------------------------|--------------------|--------------------|-----------------------------------|-----------------------------------|
| 1 | 0.9009 | 1,562,463 | 31,493 | 1,407,700 | 28,373 |
| 2 | 2.5830 | 318,871 | 20,342 | 823,650 | 52,544 |
| 3 | 0.7088 | 1,345,697 | 82,432 | 953,800 | 58,426 |
| 4 | 3.3008 | 253,657 | 23,171 | 837,270 | 76,482 |
| 5 | 1.5509 | 828,958 | 104,943 | 1,286,000 | 16,280 |

4.5 Quantitative evaluation of the brain tumor 3D visualization

3D visualization model of the brain tumor rendered from MR images is constructed from [14, 20]. Five sample cases mentioned in Table 6. These models were evaluated by five radiologists from different hospitals, having an average experience of more than 10 years in their respective fields. Prior to evaluation, radiologists were briefed about the system and were asked to rate the quality of visualization in percentage, where low percentage means low quality and vice versa. During analysis and discussion with radiologists, we reached to the conclusion that high-resolution (that is, number of voxels per mm) and number of slices are directly proportional to the quality of 3D-visualization in terms of clear structural view and volume of the tumor in the brain. The intuition taken from the analysis and rating of the radiologists are given in Table 7. The 3D visualization models of the proposed brain tumor were shown in Fig. 12. Each case was rated by five different radiologists. The average rating for case-1, case-2, case-3, case-4, and case-5 are 97.40, 94.40, 81.8, 98.4, and 88.4%, respectively, which are also shown in Table 8.

4.6 Case study: a clinical evaluation of the proposed system

Accurate detection and measurement of tumor size and its changes over time are of crucial importance for diagnosis, treatment planning, and monitoring of response to oncologic therapy for brain tumors. Brain MRI analysis is time-consuming and prone to errors due to increased measurement variability of tumor size, sensitivity to MR imaging quality, and difficulties in assessing complex and irregularly shaped brain lesions. In this context, the proposed diagnostic framework is evaluated on various patients, constituting a possible solution to the conventional MR analysis issues. In this study, tumor segmentation, volume estimation, and interactive 3D visualization results of the proposed framework were compared with manually acquired ground truth data of two expert raters for a glioblastoma (GBM) patient. GBM, also known as Grade IV Astrocytoma, is the most common and most aggressive malignant primary brain tumor in humans.

Table 4 Performance analysis of the proposed method in comparison with three other state-of-the-art classifiers, BPN [15], KNN [12], and Hybrid RGSA [26]

| Classifier | Specificity % | Sensitivity % | Accuracy % | Mean Square Error |
|-------------|---------------|---------------|------------|-------------------|
| BPN | 68.17 | 89.58 | 88.85 | 0.21 |
| KNN | 76.19 | 91.84 | 91.14 | 0.10 |
| Hybrid RGSA | 95.0 | 98.94 | 98.4 | 0.015 |
| Proposed | 95.53 | 99.49 | 99.0 | 0.09 |

Table 5 Performance results with different ranges of cross-validation for the proposed classification method

| No. of classes | Total Images | K | Cross-validation % | | Time in Seconds | | No: of features | Avg. Accuracy % | |
|----------------|--------------|----|--------------------|---------|-----------------|---------|-----------------|-----------------|---------|
| | | | Training | Testing | Training | Testing | | Training | Testing |
| 2 | 100 | 10 | 70 | 30 | 19.29 | 0.59 | 150,520 | 100 | 98.1 |
| 2 | 100 | 10 | 30 | 70 | 10.68 | 0.36 | 64,520 | 100 | 91.0 |
| 2 | 30 | 3 | 70 | 30 | 7.19 | 0.26 | 43,000 | 100 | 87.2 |
| 2 | 30 | 3 | 30 | 70 | 5.13 | 0.25 | 21,520 | 100 | 83.1 |

Table 6 Brain tumor statistics and 3D visualization accuracy

| Case No | No of slices | Voxel Size | Brain voxels | Tumor voxels | Total voxels |
|---------|--------------|------------|--------------|--------------|--------------|
| 1 | 28 | 0.7088 | 1,345,697 | 20,342 | 1,366,039 |
| 2 | 19 | 1.5509 | 828,958 | 82,432 | 911,390 |
| 3 | 17 | 2.5830 | 318,871 | 104,943 | 423,814 |
| 4 | 60 | 2.2156 | 488,853 | 0 | 488,853 |
| 5 | 28 | 2.0008 | 283,626 | 32,075 | 315,701 |

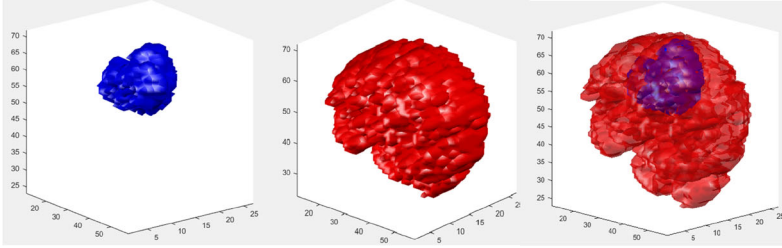
A total of 256 different MRI images for each patient were analyzed. A comparison was performed between the proposed framework, two state-of-the-art MRI analysis tools including ITK-SNAP⁴ and 3D-Doctor,⁵ and manual MRI analysis for evaluating the pros and cons of the proposed method for segmentation, classification, volume estimation, and 3D visualization. An overview of the questionnaires asked during the case study is presented in Tables 9 and 10. The studies were approved by the Local Research Ethics Commission and all methods were carried out in accordance with the approved guidelines. All patients provided written informed consent. Both raters adhered to a predefined segmentation protocol. The radiologists were given the questionnaire and different features of the proposed system were explained to them. The radiologists used the proposed system 3–4 time prior to the case study. At the start of each session, they were given one case, having 200–300 MR scans. Cases were selected to evaluate the abilities of the proposed system and to point out its weakness.

In Table 9, we examined four features of the proposed system: classification, segmentation, volume estimation, and visualization; these are important factors that affect the radiologists' ability to diagnose brain cancer. We collected radiologist responses that how a certain feature of the proposed system would facilitate medical specialist in diagnosis and treatment planning. Table 9 summarizes the two radiologists' ratings of the proposed system, ITK-SNAP, and 3D-Doctor in different perspectives. It has been observed that the proposed framework performs tumor detection, its volume estimation, and 3D visualization accurately with highly similar scores as achieved by other two MRI analysis tools. Moreover, the proposed method provides two advantages: 1) facilitates radiologist for automatic classification of huge MRI data into positive or negative cancer cases, 2) provides an open-source platform for MRI analysis where researchers can contribute in further enhancing the current framework, making it freely available for underdeveloped countries.

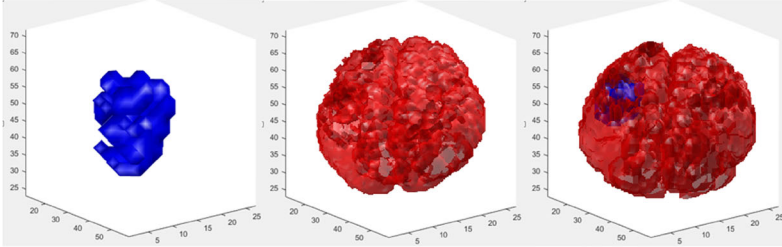
⁴ <http://www.itksnap.org/pmwiki/pmwiki.php>

⁵ <http://www.ablesw.com/3d-doctor/>

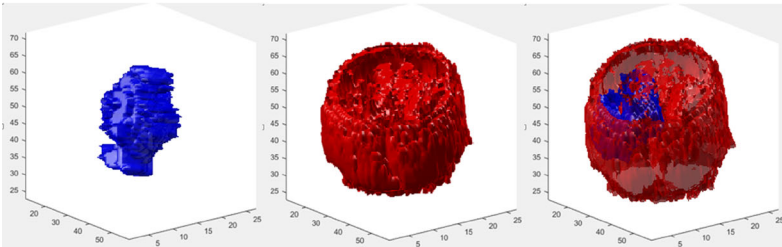
Case-(1)



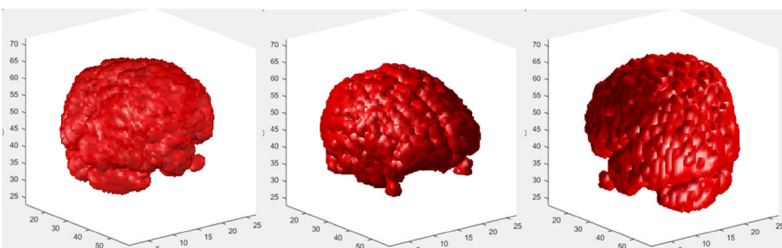
Case-(2)



Case-(3)



Case-(4)



Case-(5)

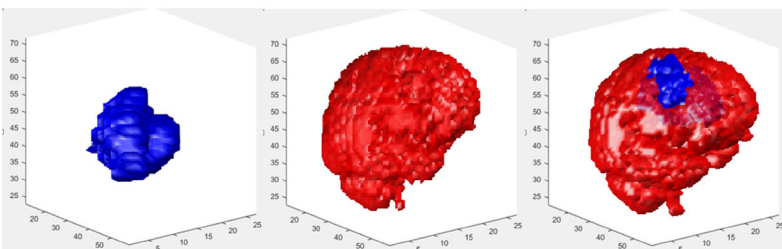


Fig. 12 Sample views of the proposed 3D visualization model for five different patients

Table 7 Radiologist list

| No. | Radiologist Name | Hospital |
|-----|--------------------|---|
| R1 | Dr. Majid | Peshawar Medical College (http://prime.edu.pk/) |
| R2 | Dr. Shandana khan | Northwest (http://www.lrh.gov.pk/) |
| R3 | Dr. Amjad Iqbal | Shaukat Khanum Memorial Cancer Hospital and research center (https://nwgh.pk/index.php) |
| R4 | Dr. Muhammad Rahim | Lady reading hospital (LRH) (http://shaukatkhanum.org.pk/) |
| R5 | Dr. Muhammad Nawaz | Hayatabad Medical Complex (HMC) (http://www.hmckp.gov.pk/) |

Software applications in the computer industry routinely undergo some type of formal usability testing. This evaluation proves important, particularly in medicine where it is applied directly to humans, making it more sensitive and highly concerned for different stakeholders. Table 10 provides usability testing questionnaire, findings, and ratings of two radiologists for the underlying proposed framework. This usability test is performed to discover the good and bad aspects of the proposed system for the purposes of design refinement and validation. It can be seen from Table 10 that the responses to the questionnaire gave positive findings and high rating scores in the perspective of usability. These studies on numerous patients found a good agreement between manual and the proposed system generated results, improving accuracy in therapy response assessment as well as reducing diagnosis time.

5 Conclusion

In this paper, an efficient framework for analysis and visualization of brain MRI is presented. Initially, a semi-automated interactive 3D segmentation method is presented which efficiently segments brain and tumor regions from underlying MR slices. This segmentation method is accurate and computationally efficient in selecting an optimal threshold value for segmentation of brain and tumor. The bow is used to extract diagnostically relevant SURF features from images and SVM is used for classification. The proposed classification model achieves high accuracy for the classification of a malignant and benign tumor as compared to other state-of-the-art methods. Finally, segmented regions are rendered using marching cube volume rendering algorithm. The marching cube method provides better rendering results and it is fast in comparison with

Table 8 Radiologist and their rating for visualization

| Radiologists | Case 1 | Case 2 | Case 3 | Case 4 | Case 5 | Average % |
|--------------|--------|--------|--------|--------|--------|-----------|
| R1 | 99 | 98 | 96 | 95 | 99 | 97.40 |
| R2 | 98 | 94 | 93 | 96 | 91 | 94.40 |
| R3 | 87 | 83 | 81 | 75 | 83 | 81.8 |
| R4 | 97 | 99 | 99 | 98 | 99 | 98.4 |
| R5 | 90 | 87 | 85 | 92 | 88 | 88.4 |

Table 9 Clinical comparative analysis of the proposed computerized decision support system with two state-of-the-art tools for brain MRI analysis

| Feature | Question | Expert Rater 1 | | Expert Rater 2 | |
|-------------------|-----------------|----------------|----------|----------------|----------|
| | | Time | Accuracy | Time | Accuracy |
| Classification | Proposed Method | + | *** | + | **** |
| | ITK-SNAP | ? | NA | ? | NA |
| | 3D-Doctor | ? | NA | ? | NA |
| Segmentation | Proposed Method | + | *** | + | *** |
| | ITK-SNAP | + | **** | +? | **** |
| | 3D-Doctor | + | **** | + | **** |
| Volume estimation | Proposed Method | + | *** | + | ** |
| | ITK-SNAP | + | *** | +? | ** |
| | 3D-Doctor | +? | **** | + | *** |
| Visualization | Proposed Method | + | *** | + | **** |
| | ITK-SNAP | + | ** | + | **** |
| | 3D-Doctor | + | *** | + | ** |

Ratings of the underlying feature quality in terms of accuracy: *poor, ** fair, ***good, ****excellent

Ratings of measurement results in terms of time complexity: (+ positive rating) fast, (– negative rating) slow, (?) indeterminate rating) medium, (+? Mixed) inconsistent behavior

NA not available

ray casting rendering algorithm. The proposed framework efficiently performs all the important processing (with minor user intervention) that is applied to biomedical imaging and have potential applications in the field of neuroimaging. Each feature of the proposed system is rigorously tested both quantitatively and qualitatively. Experimental analysis validates the efficiency of the underlying system.

The proposed framework will be extended for further classification of malignant and benign brain tumors into sub-categories, ranging from Grade I (Pilocytic Astrocytoma) to Grade IV (Glioblastoma). This will help radiologists to analyze the brain MRI in a more deep level, helping accurate diagnosis and medication. One of the possible solutions in this context could be the adoption of multi-class ensemble classifiers.

Table 10 Usability testing questionnaire for the overall subjective evaluation of the proposed MRI analysis system

| Question | Expert Rater 1 | | Expert Rater 2 | |
|---|---------------------------------------|-----------|---|-----------|
| | F | R | F | R |
| Can the results be readily used for action where necessary? | Results actionable at the local level | Good | Results actionable at both local and remote level | Excellent |
| Is the system in an easy to use format? | Easy | Excellent | Easy | Excellent |
| How long does an overall assessment take to complete? | 5 min | Excellent | 8 min | Good |
| What is the number of observations (MR images, times) needed to reach the required level of reliability for the purpose of decision making? | 50 scans, 3 times | Good | 25 scans, 4 times | Good |
| Expert perceptions of quality of the proposed system | Reliable | Good | Not sure | Not sure |

F findings, R ratings

Acknowledgments This research was supported by the Korean MSIT (Ministry of Science and ICT), under the National Program for Excellence in SW (2015-0-00938), supervised by the IITP (Institute for Information & communications Technology Promotion).

References

1. Abdellah M, Eldeib A, Sharawi A (2015) High performance GPU-based Fourier volume rendering. *Journal of Biomedical Imaging* 2015:2
2. Ahmad A, Dey L (2007) A k-mean clustering algorithm for mixed numeric and categorical data. *Data Knowl Eng* 63(2):503–527
3. Algohary AO et al (2010) Improved segmentation technique to detect cardiac infarction in MRI C-SENC images. In: *Biomedical Engineering Conference (CIBEC), 2010 5th Cairo International*. IEEE
4. Ateeq T et al (2018) Ensemble-classifiers-assisted detection of cerebral microbleeds in brain MRI. *Comput Electr Eng*
5. Bagheri MA, Montazer GA, Escalera S (2012) Error correcting output codes for multiclass classification: application to two image vision problems. In: *Artificial Intelligence and Signal Processing (AISP), 2012 16th CSI International Symposium on*. IEEE
6. Bozorgi M, Lindseth F (2015) GPU-based multi-volume ray casting within VTK for medical applications. *Int J Comput Assist Radiol Surg* 10(3):293–300
7. Chen Y-T (2012) Brain tumor detection using three-dimensional Bayesian level set method with volume rendering. In: *Wavelet Analysis and Pattern Recognition (ICWAPR), 2012 International Conference on*. IEEE
8. Dai Y et al (2013) Volume-rendering-based interactive 3D measurement for quantitative analysis of 3D medical images. *Comput Math Methods Med* 2013
9. Das AJ, Mahanta LB, Prasad V (2014) Automatic detection of brain tumor from MR Images using morphological operations and K-means based segmentation
10. Deng W et al (2010) MRI brain tumor segmentation with region growing method based on the gradients and variances along and inside of the boundary curve. In: *Biomedical Engineering and Informatics (BMEI), 2010 3rd International Conference on*. IEEE
11. Despotović I, Goossens B, Philips W (2015) MRI segmentation of the human brain: challenges, methods, and applications. *Comput Math Methods Med* 2015
12. El-Dahshan E-SA, Hosny T, Salem A-BM (2010) Hybrid intelligent techniques for MRI brain images classification. *Digital Signal Process* 20(2):433–441
13. Ghosh S, Dubey SK (2013) Comparative analysis of k-means and fuzzy c-means algorithms. *Int J Adv Comput Sci Appl*:4(4)
14. Gong F, Zhao X (2010) Three-dimensional reconstruction of medical image based on improved marching cubes algorithm. In: *Machine Vision and Human-Machine Interface (MVHI), 2010 International Conference on*. IEEE
15. Har-Peled S, Roth D, Zimak D (2003) Constraint classification for multiclass classification and ranking. In: *Advances in neural information processing systems*
16. Hohne KH (2002) Medical image computing at the institute of mathematics and computer science in medicine, university hospital hamburg-ependorf. *IEEE Trans Med Imaging* 21(7):713–723
17. Jaffar MA et al (2012) Anisotropic diffusion based brain MRI segmentation and 3D reconstruction. *International Journal of Computational Intelligence Systems* 5(3):494–504
18. Juan-Albarracín J et al (2015) Automated glioblastoma segmentation based on a multiparametric structured unsupervised classification. *PLoS One* 10(5):e0125143
19. Khotanlou H et al (2009) 3D brain tumor segmentation in MRI using fuzzy classification, symmetry analysis and spatially constrained deformable models. *Fuzzy Sets Syst* 160(10):1457–1473
20. Lorensen WE, Cline HE (1987) Marching cubes: a high resolution 3D surface construction algorithm. In: *ACM siggraph computer graphics*. ACM
21. Louis DN et al (2016) The 2016 World Health Organization classification of tumors of the central nervous system: a summary. *Acta Neuropathol* 131(6):803–820
22. Mehmood I et al (2013) Prioritization of brain MRI volumes using medical image perception model and tumor region segmentation. *Comput Biol Med* 43(10):1471–1483
23. Mehmood I, Sajjad M, Baik SW (2014) Video summarization based tele-endoscopy: a service to efficiently manage visual data generated during wireless capsule endoscopy procedure. *J Med Syst* 38(9):109

24. Mehmood I, Sajjad M, Baik SW (2014) Mobile-cloud assisted video summarization framework for efficient management of remote sensing data generated by wireless capsule sensors. *Sensors* 14(9):17112–17145
25. Natarajan P et al (2012) Tumor detection using threshold operation in MRI brain images. In: *Computational Intelligence & Computing Research (ICCIC)*, 2012 I.E. International Conference on. IEEE
26. Rajesh Sharma R, Marikkannu P (2015) Hybrid RGSA and support vector machine framework for three-dimensional magnetic resonance brain tumor classification. *Sci World J*:2015
27. Ray D, Majumder DD, Das A (2012) Noise reduction and image enhancement of MRI using adaptive multiscale data condensation. In: *Recent Advances in Information Technology (RAIT)*, 2012 1st International Conference on. IEEE
28. Vrji KA, Jayakumari J (2011) Automatic detection of brain tumor based on magnetic resonance image using CAD System with watershed segmentation. In: *Signal Processing, Communication, Computing and Networking Technologies (ICSCCN)*, 2011 International Conference on. IEEE
29. Wang T, Cheng I, Basu A (2010) Fully automatic brain tumor segmentation using a normalized Gaussian Bayesian classifier and 3D fluid vector flow. In: *Image Processing (ICIP)*, 2010 17th IEEE International Conference on. IEEE
30. Yang G et al (2016) Automated classification of brain images using wavelet-energy and biogeography-based optimization. *Multimedia Tools and Applications* 75(23):15601–15617
31. Yazdani S et al (2014) Magnetic resonance image tissue classification using an automatic method. *Diagn Pathol* 9(1):207
32. Zakeri FS, Behnam H, Ahmadinejad N (2012) Classification of benign and malignant breast masses based on shape and texture features in sonography images. *J Med Syst* 36(3):1621–1627
33. Zhang H et al (2011) An automated and simple method for brain MR image extraction. *Biomed Eng Online* 10(1):81
34. Zhang Y-D, Yuan T-F, Dong Z-C (2017) Brain imaging and automatic analysis in neurological and psychiatric diseases—part I. *CNS & Neurological Disorders-Drug Targets (Formerly Current Drug Targets-CNS & Neurological Disorders)* 16(1):3–4



Irfan Mehmood received BS degree in Computer Science in 2010 from National University of Computer and Emerging Sciences, Pakistan. From 2010 to 2011, he served as a Software Engineer in Talented Earth Organization, where he provided various services such as mobile application development. At the end of 2011, he joined Intelligent Media Laboratory (IM Lab) as a research associate while enrolling as a PhD student in Sejong University, Seoul, South Korea. In IM Lab, he worked on various projects related to video summarization and prioritization, image super-resolution, image quality assessment, and mixed reality. In 2016, he joined Sejong University South Korea and serving as an assistant professor in Software department. He is also head of Visual Analytics Lab, where students are working on research projects such social data mining and information retrieval, steganography, digital watermarking, and medical imaging analysis etc. under his supervision. His current research activities include social data mining, multi-modal medical data analysis, information summarization and multi-modal surveillance frameworks.



Muhammad Sajjad received his Master degree from Department of Computer Science, College of Signals, National University of Sciences and Technology, Rawalpindi, Pakistan. He received his Ph.D. degree in Digital Contents from Sejong University, Seoul, Republic of Korea. He is now working as an assistant professor at Department of Computer Science, Islamia College Peshawar, Pakistan. He is also head of “Digital Image Processing Laboratory (DIP Lab)” at Islamia College Peshawar, Pakistan, where students are working on research projects such social data analysis, medical image analysis, multi-modal data mining and summarization, image/video prioritization and ranking, Fog computing, Internet of Things, virtual reality, and image/video retrieval under his supervision. His primary research interests include computer vision, image understanding, pattern recognition, and robot vision and multimedia applications, with current emphasis on raspberry-pi and deep learning-based bioinformatics, video scene understanding, activity analysis, Fog computing, Internet of Things, and real-time tracking.



Khan Muhammad (S’16) received the bachelor’s degree in computer science from the Islamia College Peshawar, Pakistan, with a focus on information security. He is currently pursuing the M.S. leading to Ph.D. degree in digital contents from Sejong University, Seoul, South Korea. He has been a Research Associate with the Intelligent Media Laboratory since 2015. He has authored over 40 papers in peer-reviewed international journals and conferences, such as IEEE Transactions on Industrial Informatics, IEEE Transactions on SMC-Systems, the IEEE Access, Neurocomputing, Future Generation Computer Systems, Pattern Recognition Letters, Computers in Industry, PLOS ONE, the Journal of Medical Systems, Biomedical Signal Processing and Control, Multimedia Tools and Applications, Pervasive and Mobile Computing, SpringerPlus, the KSII Transactions on Internet and Information Systems, MITA 2015, PlatCon 2016, FIT 2016, Platcon-17 and ICNGC-2017. His research interests include image and video processing, information security, image steganography, video summarization,

diagnostic hysteroscopy, wireless capsule endoscopy, computer vision, deep learning, and video surveillance. He is an active reviewer of more than 40 reputed journals and is involved in editing of several special issues.



Syed Inayat Ali Shah received his M.Phil degree from Quaide-Azam University Islamabad, Pakistan in 1990 and Ph.D. degree from Saga University Japan in 2002. He is currently working as Professor of Mathematics and Dean Faculty of Physical & Numerical Science, Islamia College Peshawar, Pakistan. His research interest includes fuzzy theory, computing, number theory, modeling & simulation and image processing.



Arun Kumar Sangaiah has received his Doctor of Philosophy (PhD) degree in Computer Science and Engineering from the VIT University, Vellore, India. He is presently working as an Associate Professor in School of Computer Science and Engineering, VIT University, India. His area of interest includes software engineering, computational intelligence, wireless networks, bio-informatics, and embedded systems. He has authored more than 100 publications in different journals and conference of national and international repute. His current research work includes global software development, wireless ad hoc and sensor networks, machine learning, cognitive networks and advances in mobile computing and communications. Also, he was registered a one Indian patent in the area of Computational Intelligence. Besides, Prof. Sangaiah is responsible for Editorial Board Member/Associate Editor of various international journals.



Muhammad Shoib received his BCS degree from International Islamic University, Islamabad, Pakistan in the field of computer science. Currently, he is doing Master degree in computer science from Islamia College Peshawar, Pakistan. He is an active member of Digital Image Processing Lab, Department of Computer Science, Islamia College Peshawar. His research interests include medical image processing, segmentation, classification and healthcare services.



Sung Wook Baik received the B.S degree in computer science from Seoul National University, Seoul, Korea, in 1987, the M.S. degree in computer science from Northern Illinois University, Dekalb, in 1992, and the Ph.D. degree in information technology engineering from George Mason University, Fairfax, VA, in 1999. He worked at Datamat Systems Research Inc. as a senior scientist of the Intelligent Systems Group from 1997 to 2002. In 2002, he joined the faculty of the College of Electronics and Information Engineering, Sejong University, Seoul, Korea, where he is currently a Full Professor and Dean of Digital Contents. He is also the head of Intelligent Media Laboratory (IM Lab) at Sejong University. His research interests include computer vision, multimedia, pattern recognition, machine learning, data mining, virtual reality, and computer games.